Optim Eng (2006) 7:297–316
DOI 10.1007/s11081-006-9973-8

# A study using Monte Carlo Simulation for failure probability calculation in Reliability-Based Optimization

**Dhanesh Padmanabhan · Harish Agarwal · John E. Renaud · Stephen M. Batill**

Received: 10 June 2004 / Revised: 3 May 2005


**Abstract** In this study, a Reliability-Based Optimization (RBO) methodology that uses Monte Carlo Simulation techniques, is presented. Typically, the First Order Reliability Method (FORM) is used in RBO for failure probability calculation and this is accurate enough for most practical cases. However, for highly nonlinear problems it can provide extremely inaccurate results and may lead to unreliable designs. Monte Carlo Simulation (MCS) is usually more accurate than FORM but very computationally intensive. In the RBO methodology presented in this paper, limit state approximations are used in conjunction with MCS techniques in an approximate MCS-based RBO that facilitates the efficient calculation of the probabilities of failure. A FORM-based RBO is first performed to obtain the initial limit state approximations. A Symmetric Rank-1 (SR1) variable metric algorithm is used to construct and update the quadratic limit state approximations. The approximate MCS-based RBO uses a conditional-expectation-based MCS, that was chosen over indicator-based MCS because of the smoothness of the probability of failure estimates and the availability of analytic sensitivities. The RBO methodology was implemented for an analytic test problem and a higher-dimensional, control-augmented-structure test problem. The results indicate that the SR1 algorithm provides accurate limit state approximations (and therefore accurate estimates of the probabilities of failure) for these test problems. It was also observed that the RBO methodology required two orders of magnitude fewer analysis calls than an approach that used exact limit state evaluations for both test problems.

**Keywords** Reliability analysis · Reliability-Based Optimization · Monte Carlo Simulation · Importance sampling

D. Padmanabhan (✉) · H. Agarwal · J. E. Renaud · S. M. Batill
Department of Aerospace and Mechanical Engineering, University of Notre Dame, Notre Dame, IN 46556, USA
e-mail: dhanesh123us@gmail.com

## 1 Introduction

In a traditional design optimization, the design variables and other system parameters are usually considered as deterministic inputs. The design obtained by performing a deterministic design optimization is usually limited by selected design constraints, leaving little or no latitude for uncertainties. The resulting deterministic optimum has a high probability of violating the design constraints, due to the influence of uncertainties inherently present during the modelling and manufacturing phases of the artifact and due to uncertainties in the operating environment of the artifact. These uncertainties include variations in certain parameters (e.g., dimensions, material properties, loads), and model uncertainties and errors associated with the numerical analysis tools used for simulation-based design (Oberkampf et al., 2000). In this paper, uncertainties are modelled as continuous random variables. In applications such as the design of structures, many of the design constraints represent various failure modes such as yielding, buckling, fatigue, collapse etc. Designs resulting from deterministic optimization can be unreliable and might lead to catastrophic failure. Uncertainties in simulation-based design are inherently present and need to be accounted for in the design optimization process. Reliability-Based Optimization (RBO) is a methodology that addresses this problem.

Reliability-Based Optimization (RBO) (Enevoldsen and Sørensen, 1994) is usually expressed in a form where one is required to minimize a cost function subject to certain reliability (i.e. probabilistic) constraints and deterministic constraints. The reliability constraints ensure that the probabilities of failure with respect to various failure modes are below acceptable levels. The probabilities of failure are usually obtained using standard reliability analysis methods (Haldar and Mahadevan, 2000; Ditlevsen and Madsen, 1996) like the First Order Reliability Methods (FORM), the Second Order Reliability Methods (SORM), and Monte Carlo Simulation (MCS) techniques. The application of most of these reliability methods require the computation of a Most Probable Point (MPP). FORM and SORM are based on linear and quadratic approximations of the limit state functions at the MPP, respectively. RBO is typically performed with FORM-based reliability constraints. Variations of FORM-based RBO have been proposed by researchers (Tu and Choi, 1999; Kirjner-Neto et al., 1998; Kuschel and Rackwitz, 1997) that address the issues of computational cost and poor robustness of traditional optimization methods used for FORM analysis. Approximation concepts have also been been used to address the issue of computational cost for FORM-based RBO (Grandhi and Wang, 1998). FORM has been observed to perform well for many practical design applications. But the probability of failure estimated using FORM, can be inaccurate (either under-conservative or over-conservative) and might lead to unacceptable designs, especially for nonlinear problems with low or medium reliability.

MCS techniques are typically more accurate than FORM. The major difficulty in using MCS techniques is that they can be computationally expensive. Moreover, most MCS techniques cannot be incorporated within a gradient-based optimizer for RBO, because of the unavailability of analytic sensitivities and non-smoothness of probability of failure estimates with design changes. In RBO, the probabilities of failure corresponding to the failure modes have to be computed at a number of designs visited by the optimizer. Therefore, using MCS techniques directly with the simulation tools,

assumed to be expensive themselves, is highly impractical. There are some studies that incorporate MCS techniques in RBO in an efficient manner using approximation concepts (Oakley et al., 1998) but they do not address the issue of suitability of MCS techniques for RBO using gradient-based optimizers. The study presented in this paper deals with the selection of MCS techniques for RBO and the development of RBO methodologies that incorporate these techniques in a computationally efficient manner using approximation concepts.

## 2 Reliability-Based Optimization

Reliability-Based Optimization (RBO) is a methodology of finding optimum designs, characterized by a low probability of failure. A typical RBO formulation involves the minimization of a cost function (e.g., weight of a structure) subject to reliability constraints and certain deterministic constraints. This can be mathematically represented by

$$\min_{\mathbf{d}} \quad f(\mathbf{d}, \mathbf{p}), \tag{1}$$

$$\text{s.t.} \quad \mathbf{g}^{\text{rbo}}(\mathbf{d}, \mathbf{p}) \geq 0, \tag{2}$$

$$g_j^D(\mathbf{d}, \mathbf{p}) \geq 0 \quad \text{for } j = 1, \ldots, M_D, \tag{3}$$

$$\text{Bounds:} \quad \mathbf{d}_l \leq \mathbf{d} \leq \mathbf{d}_u, \tag{4}$$

where $\mathbf{d}$ is the vector consisting of unknown design variables and $\mathbf{p}$ is the vector consisting of fixed parameters of the optimization problem. $f$ is the cost function, $g_j^D$ is the $j$th deterministic constraint and $M_D$ is the number of deterministic constraints. Deterministic constraints arise from other design considerations such as cost, marketing etc. $\mathbf{g}^{\text{rbo}}$ represent constraints on reliability indices with respect to various component failure modes or a single constraint on reliability index for an overall system failure mode. The overall system failure mode can be a series, parallel or a combination of series and parallel of all the component failure modes (Enevoldsen and Sørensen, 1993). There are also other system failure criteria, for example a case where a system is said to have failed if K out of N components fail. The discussion in this paper will be restricted to reliability constraints with component failure modes alone. The component failure modes are represented by limit state functions, $g_i^R, i = 1, \ldots, M_R$, where $M_R$ is the number of component failure modes. Examples of limit state functions are stress constraints, frequency constraints and structural displacement constraints. If $g_i^R < 0$, failure has occurred with respect to the $i$th component failure mode and vice-versa, if $g_i^R > 0$ the failure has not occurred. $g_i^R = 0$ is usually referred to as the limit state. In a deterministic design optimization, where uncertainties are not considered, these limit state functions are treated as deterministic constraints. The component reliability constraints are constraints on the reliability indices corresponding to the component failure modes. The reliability techniques used to compute these reliability indices are discussed in the next section. The component reliability constraints are given by the

following equation:

$$g_i^{\text{rbo}} = \beta_i - \beta_{\text{reqd},i} \quad \text{for } i = 1, \ldots, M_R, \tag{5}$$

where $\beta_i$ is the reliability index and $\beta_{\text{reqd,i}}$ is the required reliability index corresponding to the $i$th failure mode. The reliability index is directly related to the corresponding probability of failure as $P_i = \Phi(-\beta_i)$, where $\Phi$ is the one-dimensional Gaussian cumulative distribution function. The reliabilty index is inversely proportional to the probability of failure.

### 2.1 Reliability analysis

Standard reliability techniques are required to estimate the probabilities of failure (Haldar and Mahadevan, 2000; Ditlevsen and Madsen, 1996). In these techniques, the uncertainties are modelled as continuous random variables, $X_1, X_2, \ldots, X_n$ with known joint probability density function. The uncertain variables can be denoted by the vector $\mathbf{X}$, where $\mathbf{X} = \{X_1, X_2, \ldots, X_n\}$. $\mathbf{x} = \{x_1, x_2, \ldots, x_n\}$ denotes an instantiation of random vector $\mathbf{X}$ and equivalently $x_1, x_2, \ldots, x_n$ denote joint instantiations of random variables $X_1, X_2, \ldots, X_n$ respectively. The joint probability density function (PDF) of all the random variables is given by $f_{\mathbf{X}}(\mathbf{x}; \boldsymbol{\theta})$, where $\boldsymbol{\theta}$ is a vector whose elements are distribution parameters such as means, modes, standard deviations and coefficients of variation of $\mathbf{X}$. $\boldsymbol{\theta}$ consist of variable distribution parameters, $\boldsymbol{\theta}^d$, that the designer is allowed to vary, and fixed distribution parameters, $\boldsymbol{\theta}^p$. The elements of the design vector, $\mathbf{d}$, consist of the variable distribution parameters and other variables, $\boldsymbol{\eta}$. $\mathbf{p}$ consist of the fixed distribution parameters and other fixed parameters, $\mathbf{p}^m$. Mathematically, the relationships among $\boldsymbol{\theta}$, $\mathbf{d}$, $\mathbf{p}$ and $\boldsymbol{\eta}$ can be represented by the following equations:

$$\boldsymbol{\theta} = \{\boldsymbol{\theta}^d, \boldsymbol{\theta}^p\}, \tag{6}$$

$$\mathbf{d} = \{\boldsymbol{\theta}^d, \boldsymbol{\eta}\}, \tag{7}$$

$$\mathbf{p} = \{\boldsymbol{\theta}^p, \mathbf{p}^m\}. \tag{8}$$

The $i$th limit state function is denoted as $g_i^R(\mathbf{X}, \boldsymbol{\eta})$. The probability of failure due to the $i$th component failure mode is $P_i = P(g_i^R(\mathbf{X}, \boldsymbol{\eta}) < 0)$. The subscript for $g^R$ will be dropped in the remainder of this section and next section for convenience. It has to be noted that the following discussions are valid for each limit state function.

In FORM, SORM, and some of the MCS techniques, the following procedures are typically performed, which involve the calculation of a Most Probable Point (MPP) in a transformed random variable space:

1. The original random variable vector, $\mathbf{X}$ is transformed to a standard normal independent random variable vector, $\mathbf{U}$, by a one-to-one transformation $\mathbf{T}$ (i.e. $\mathbf{U} = \mathbf{T}(\mathbf{X}, \boldsymbol{\theta})$). A Rosenblatt transformation is typically used to transform the random variables (Rosenblatt, 1952). The limit state function in the $\mathbf{u}$ space will be denoted as $g^R(\mathbf{u}, \boldsymbol{\eta})$.

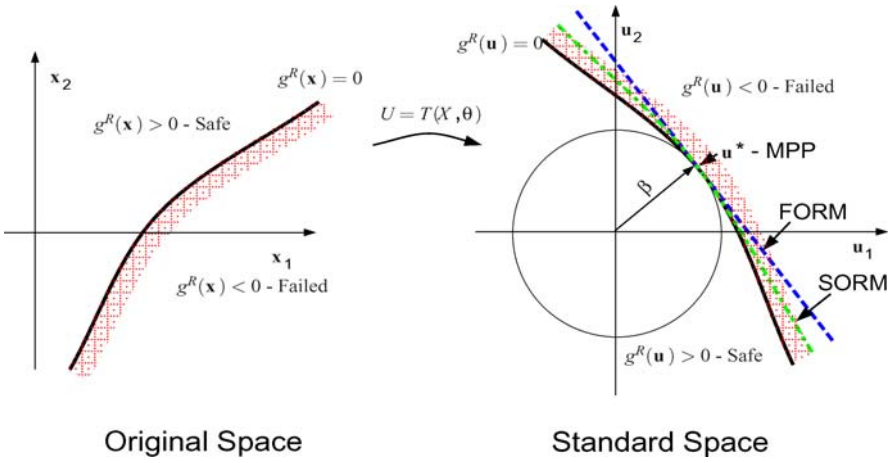


**Fig. 1** Illustration of original to standard space transformation and MPP, FORM reliability index and FORM and SORM approximations in standard space

2. A Most Probable Point (MPP) of failure, $\mathbf{u}^*$, is found by solving the following optimization problem:

$$\min_{\mathbf{u}} \ \mathbf{u}^T\mathbf{u}, \tag{9}$$

$$\text{s.t.} \ \ g^R(\mathbf{u}, \boldsymbol{\eta}) = 0. \tag{10}$$

$\mathbf{u}^*$ is the point on the $g^R(\mathbf{u}, \boldsymbol{\eta}) = 0$ surface that is closest to the origin. The $g^R(\mathbf{u}, \boldsymbol{\eta}) = 0$ surface is usually referred to as a limit state surface and its evaluation requires the computation of the inverse transformation, $\mathbf{T}^{-1}$.

Figure 1 illustrates the transformation of the limit state function and the associated failure domain from original space to standard space and also illustrates the MPP in standard space for an example with two random variables, $X_1$ and $X_2$. Various algorithms exist to perform the MPP searches (Liu and Der Kiureghian, 1991). One of the approaches is the Hasofer-Lind and Rackwitz-Fiessler (HL-RF) algorithm that is based on a Newton-Raphson root solving approach. Variants of the HL-RF method exist that use additional line searches. The family of HL-RF algorithms can exhibit poor convergence for highly nonlinear and badly scaled problems, since they are based on a first order approximation of the limit state function. A Sequential Quadratic Programming (SQP) approach is often a more robust approach since it is based on a second order approximation of the limit state function. Moreover, SQP has been successfully applied to various nonlinear optimization problems and is readily available in many optimization packages. Hence, SQP has been chosen for the implementation studies presented in this paper. FORM and SORM are based on first and second order approximations of the limit state surface respectively. The magnitude of the FORM reliability index equals the distance of the MPP from the origin. Figure 1 shows the approximations corresponding to FORM and SORM in the standard space and also the FORM reliability index, $\beta$.

RBO with FORM-based reliability constraints can be easily implemented using a standard gradient-based optimizer because the reliability indices and their sensitivities can be easily computed at a given design, **d**, as given in the following steps:

1. The FORM reliability index is computed using the following equation:

$$\beta = \frac{-\nabla_u g^R}{\|\nabla_u g^R\|}\mathbf{u}^*. \tag{11}$$

2. The analytic sensitivities of $\beta$ with respect to $\boldsymbol{\theta}$ and $\boldsymbol{\eta}$ is computed using the following equations:

$$\frac{\partial \beta}{\partial \boldsymbol{\theta}} = -\frac{\nabla_u g^R(\mathbf{u}^*)}{\|\nabla_u g^R(\mathbf{u}^*)\|}\frac{\partial T(\mathbf{x}^*, \boldsymbol{\theta})}{\partial \theta}, \tag{12}$$

$$\frac{\partial \beta}{\partial \boldsymbol{\eta}} = \frac{1}{\|\nabla_u g^R(\mathbf{u}^*)\|}\frac{\partial g^R(\mathbf{u}^*, \boldsymbol{\eta})}{\partial \eta}. \tag{13}$$

The analytic sensitivities of FORM reliability index and the corresponding reliability constraint with respect to **d** is given by the following equation:

$$\frac{\partial g^{\text{rbo}}}{\partial \mathbf{d}} = \frac{\partial \beta}{\partial \mathbf{d}} = \left\{\frac{\partial \beta}{\partial \boldsymbol{\theta}^d}, \frac{\partial \beta}{\partial \boldsymbol{\eta}}\right\}. \tag{14}$$

The probability of failure obtained from FORM can be inaccurate for cases where the limit state surfaces are highly nonlinear due to nonlinearity of the transformation, **T**. The inaccuracy in a FORM estimate usually tends to be larger for problems with low or medium reliability ($\beta \approx 2$–$3$). One of the extreme cases is the inaccuracy of FORM reliability index due to the existence of multiple MPPs for a given limit state. Another extreme case involves the counter-intuitive sensitivities of the FORM reliability index with respect to standard deviations of random variables for certain asymmetrical distribution types (Sørensen and Enevoldsen, 1993). One can obtain better accuracy with SORM in some of the cases, but in general MCS techniques are the most accurate of these techniques.

## 3 Monte Carlo Simulation techniques

A general expression for the probability of failure, $P$, is given by the multidimensional integral

$$P = \int_{\Omega_f} f_{\mathbf{Z}}(\mathbf{z})\, d\mathbf{z}, \tag{15}$$

where $\Omega_f$ is the failure region, **Z** is the random or uncertain variable vector in either the original space or the standard space, i.e. **Z** is either **X** or **U** and $f_{\mathbf{Z}}$ is the joint probability density function. $\Omega_f$ is given by $g^R(\mathbf{z}, \boldsymbol{\eta}) < 0$ for a single failure mode

or component. MCS techniques estimate $P$ given by Equation (15) by randomly generating samples according to some sampling density function. A traditional way to estimate $P$ would be to use $f_{\mathbf{Z}}$ as the sampling density function. The estimate of $P$, denoted as $\hat{P}$, obtained using such a traditional approach can be given by the following equation:

$$\hat{P} = \frac{1}{N} \sum_{i=1}^{N} I(g^R(\mathbf{z}_i) < 0). \tag{16}$$

In the above equation $N$ is the number of sample points, $I$ is the indicator function (1 if $g^R < 0$, 0 otherwise) and $\mathbf{z}_i$ for $i = 1, \ldots, N$ are the sample points generated according to $f_{\mathbf{Z}}$. The number of samples required to estimate $P$ using such an approach with a reasonable accuracy is usually very high because $P$ is typically in the range $10^{-2} - 10^{-6}$. $P$ can be efficiently estimated using Quasi Monte Carlo techniques where sampling is done in important regions in $\mathbf{z}$. The important regions include regions in the failure domain that contribute significantly to the probability of failure. Example of an important region is a region centered around the MPP of a limit state function. Quasi MCS techniques can be classified as indicator-based MCS and conditional-expectation-based MCS. In the following, a brief description of these two classes of MCS techniques will be provided and some remarks on obtaining analytic sensitivities of probabilities of failure will be made.

### 3.1 Indicator-based MCS

In indicator-based MCS techniques (Engelund and Rackwitz, 1993; Bjerager, 1989), random samples of a simulation variable, $\mathbf{V}$, is generated according to a sampling density $h_{\mathbf{V}}$ such that the samples are generated in important regions in $\mathbf{z}$ space that have major contributions to $P$. Hence $P$ and its estimate, $\hat{P}$, for a single failure mode or component can be written as follows:

$$P = \int_{g^R<0} \frac{f_{\mathbf{Z}}(\mathbf{z}(\mathbf{v}))}{h_{\mathbf{V}}(\mathbf{v})} h_{\mathbf{V}}(\mathbf{v})\, d\mathbf{v}, \tag{17}$$

$$\hat{P} = \frac{1}{N} \sum_{i=1}^{N} I\left(g^R(\mathbf{z}(\mathbf{v}_i)) < 0\right) \frac{f_{\mathbf{Z}}(\mathbf{z}(\mathbf{v}_i))}{h_{\mathbf{V}}(\mathbf{v}_i)}. \tag{18}$$

In the above equation, $\mathbf{v}_i$ denote the $i$th random sample of the random vector $\mathbf{V}$ and $\mathbf{z}(\mathbf{v}_i)$ denote the corresponding sample transformed to the $\mathbf{z}$ space or coordinates. An example of an indicator-based importance sampling method involves sampling around the MPP of $g^R(\mathbf{u}, \boldsymbol{\eta})$ according to some sampling density function $h_{\mathbf{V}}$.

In an RBO driven by a gradient-based optimizer, sensitivities of $P$ are required with respect to the distribution parameters, $\boldsymbol{\theta}^d$, and deterministic parameters, $\boldsymbol{\eta}$, that form the design variable vector, $\mathbf{d}$. Sensitivities of $P$ using finite differences will require repetitions of the MCS and is computationally expensive. It is also not easy to obtain accurate sensitivities using finite differences because of the discontinuities of probability of failure that arise with changes in design. This issue will be explained

later in this section. For indicator-based MCS, the sensitivity of $P$ with respect to $\boldsymbol{\theta}$ can be easily obtained in $\mathbf{X}$ space since the failure domain is independent of $\boldsymbol{\theta}$ in this space. This can be obtained by analytically differentiating Equation (15) and evaluating the resulting multidimensional integral using the same sampling density function and samples. On the other hand, the sensitivity of $P$ with respect to $\boldsymbol{\eta}$ is given by the surface integral

$$\frac{\partial P}{\partial \boldsymbol{\eta}} = -\int_{g^R(\mathbf{z},\boldsymbol{\eta})=0} \frac{\partial g^R}{\partial \boldsymbol{\eta}} \frac{f_{\mathbf{Z}}}{\|\nabla_z g^R\|} \, d\mathbf{z}. \tag{19}$$

The above integral is performed on the limit state surface $g^R(\mathbf{z}, \boldsymbol{\eta}) = 0$. This cannot be performed using the existing samples in most of the indicator-based MCS approaches, since the samples do not lie on this surface. The adaptive importance sampling technique (Maes et al., 1993) is an exception where the limit state surface is approximated as a paraboloid and the sampling densities are picked in such a way that the surface integral can be performed in the curvilinear co-ordinates of the paraboloid. It should be noted though that the sensitivity is based on an approximation of the limit state surface.

A major issue that arises in applying these techniques in an RBO is that there are discontinuities in the probability of failure estimates with changes in design variables. This will present problems when performing an RBO using a gradient-based optimizer. The discontinuities of probability of failure can be reduced to some extent by eliminating the variations due to a varying number of sample points or varying seed of the random number generator by fixing the number of sample points and the seed to some initial state. But significant discontinuities in probability of failure will still arise due to changes in curvature of the limit state surface with design changes. This results in shifting of sample points across the limit state surface that causes discrete jumps or drops in probability of failure estimates. Figure 2 illustrates the shifting of sample points arising due to change in curvature of the limit state surface, for a case where the sampling is performed at the MPP of the limit state surface and the number of simulations and seed is not changed. To facilitate the illustration, the $\mathbf{z}$ co-ordinates

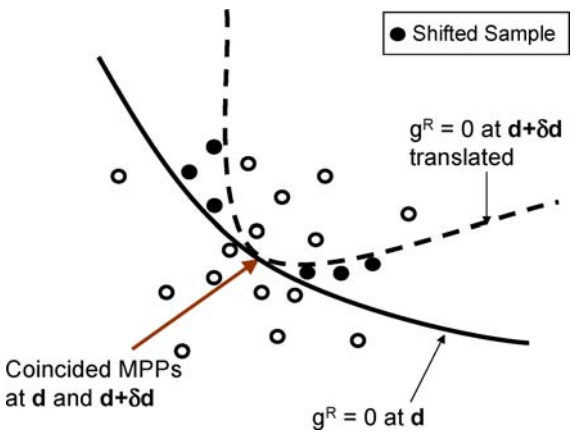


**Fig. 2** Illustration of shifting of importance-sampling based MCS samples across limit state that changes curvature with change in design. The $\mathbf{z}$ co-ordinates at the perturbed design, $\mathbf{d} + \delta\mathbf{d}$ has been translated such that the MPPs and samples coincide with the original design $\mathbf{d}$

at the perturbed design, $\mathbf{d} + \delta\mathbf{d}$ has been translated such that the MPPs and samples coincide with the MPPs and samples at the original design $\mathbf{d}$.

### 3.2 Conditional-expectation-based MCS

There are other MCS techniques that are based on conditional expectations (Bjerager, 1989; Ditlevsen and Madsen, 1996), for example directional simulation and axis orthogonal simulation. These methods are typically performed in $\mathbf{u}$-space. In the current paper, axis orthogonal simulation was used and hence will be discussed in some detail. In an Axis-Orthogonal Simulation, the following steps are carried out for the calculation of failure probability for a single failure mode:

1. MPP of the limit state function is computed.
2. A new co-ordinate system $\{\mathbf{v}, v_n\}$ is obtained by a linear or affine transformation of $\mathbf{u}$-space. This transformation is also used to transform the random variables $\mathbf{U}$ to $\{\mathbf{V}^\dagger, V_n\}$. The simulation variable $\mathbf{V}$ is defined in $\mathbf{v}$ space (which is $n-1$ dimensional) and the sampling density is $h_{\mathbf{V}}$. It should be noted that $\mathbf{V}^\dagger$ and $\mathbf{V}$ are different random variables. For a single failure mode, the $v_n$ axis is picked such that it coincides with the vector joining the origin and the MPP, see Figure 3. The linear transformation from $\mathbf{u}$ to $\{\mathbf{v}, v_n\}$ can be accomplished by a Gram-Schmidt Orthogonalization process.
3. $P$ is computed by sampling in $\mathbf{V}$ according to sampling density $h_{\mathbf{V}}$ and by performing an exact integral in $v_n$ conditioned on $\mathbf{V} = \mathbf{v}$. $P$ and estimate of $P$ are given by the following equations:

$$P = \int_{\mathbb{R}^{n-1}} \left[ \int_{g^R<0} f_{V_n}(v_n|\mathbf{v})\, dv_n \right] \frac{f_{\mathbf{V}^\dagger}(\mathbf{v})}{h_{\mathbf{V}}(\mathbf{v})} h_{\mathbf{V}}(\mathbf{v})\, d\mathbf{v}, \tag{20}$$

$$\hat{P} = \frac{1}{N} \sum_{i=1}^{N} \left[ \int_{g^R<0} f_{V_n}(v_n)\, dv_n \right] \frac{f_{\mathbf{V}^\dagger}(\mathbf{v}_i)}{h_{\mathbf{V}}(\mathbf{v}_i)}. \tag{21}$$

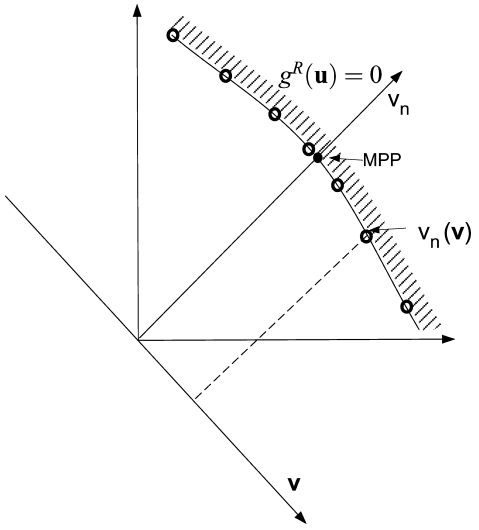


**Fig. 3** Illustration of axis orthogonal simulation in standard space showing the $\{\mathbf{v}, v_n\}$ co-ordinates and the projection $v_n(\mathbf{v})$ corresponding to a sample point $\mathbf{v}$

The integral in $v_n$ is a one dimensional integral. This is computed by solving for the roots of $g^R(\{\mathbf{v}_i, v_n\}) = 0$ for each sample $\mathbf{v}_i$. The root solving can be done using a Newton-Raphson scheme. The interval in which the root is to be located can be chosen such that it corresponds to a range of high probability level, say 0 to 6. One systematic way to select the upper bound of the interval is to make sure that the error obtained in the probability estimate calculation by neglecting the solutions outside this range is a small fraction, say 0.01, of the probability corresponding to the required reliability sought. So if $\kappa$ is the upper bound, $\kappa$ can be calculated using the relation $\Phi(-\kappa) = 0.01\Phi(-\beta_{\text{reqd}})$. It is possible to have cases with more than a single solution, but only a single solution is assumed in the current study. The root solving is equivalent to projecting the sample points along $v_n$ axis. If a single root exists for the root solving problem and if $\mathbf{V}$ is chosen as a standard normal random variables then the estimate of probability of failure can be given by following equation:

$$\hat{P} = \frac{1}{N}\sum_{i=1}^{N}\left(1 - \Phi\left(v_n(\mathbf{v}_i)\right)\right). \tag{22}$$

Unlike the indicator-based MCS techniques, discontinuities due to "shifting" of sample points across the limit state surface are absent for this MCS technique, assuming that the number of samples and the seeds are fixed. But discontinuities can still arise especially when there is a change in the number of samples that are projectable onto the limit state surface. This happens when the solution of the 1-D root solving problem, for a given sample, is also a local minimum for $g^R$ along the direction $v_n$. The magnitude of variation in a probability of failure estimate mainly depends on the magnitude of $v_n$ at which this discontinuity arises. The larger this value, the smaller the variation. These discontinuities are usually milder than the discontinuities that arise in indicator-based MCS techniques.

Unlike the indicator-based MCS techniques, all the sample points are strictly projected onto the limit state surface in the axis orthogonal simulation and consequently the sensitivities of $\hat{P}$ can be easily obtained. Hence axis orthogonal simulation was selected as the MCS technique in this study. The sensitivities of $\hat{P}$ with respect to $\mathbf{d}$, $\frac{\partial \hat{P}}{\partial \mathbf{d}}$ depend on $\frac{\partial v_n(\mathbf{v}_i)}{\partial \mathbf{d}}$ and is given by the following equation:

$$\frac{\partial \hat{P}}{\partial \mathbf{d}} = \frac{-1}{N}\sum_{i=1}^{N}\left(\phi\left(v_n(\mathbf{v}_i)\right)\frac{\partial v_n(\mathbf{v}_i)}{\partial \mathbf{d}}\right), \tag{23}$$

where $\phi$ is the one-dimensional Gaussian density function. $\frac{\partial v_n(\mathbf{v}_i)}{\partial \mathbf{d}}$ depend on the sensitivities of $g^R$, with respect to $\mathbf{d}$, evaluated at $\mathbf{u}(\mathbf{v}_i, v_n)$. $\frac{\partial v_n(\mathbf{v}_i)}{\partial \mathbf{d}}$ is comprised of $\frac{\partial v_n(\mathbf{v}_i)}{\partial \boldsymbol{\theta}^d}$ and $\frac{\partial v_n(\mathbf{v}_i)}{\partial \boldsymbol{\eta}}$, which are given by the following equations:

$$\frac{\partial v_n(\mathbf{v}_i)}{\partial \boldsymbol{\theta}^d} = \frac{\nabla_u g^R \frac{\partial T}{\partial \boldsymbol{\theta}^d}}{\left(\nabla_u g^R \frac{\partial \mathbf{u}(\mathbf{v}_i, v_n)}{\partial v_n}\right)}, \tag{24}$$

$$\frac{\partial v_n(\mathbf{v}_i)}{\partial \boldsymbol{\eta}} = \frac{-\frac{\partial g^R}{\partial \eta}}{\left(\nabla_u g^R \ \frac{\partial \mathbf{u}(\mathbf{v}_i, v_n)}{\partial v_n}\right)}. \tag{25}$$

It has to be noted that the same sample points are used for computing these sensitivities. Since the probability of failure and reliability index are related by $\hat{P} = \Phi(-\beta)$, one can compute the sensitivities of reliability index and reliability constraints using the following relation:

$$\frac{\partial g^{\text{rbo}}}{\partial \mathbf{d}} = \frac{\partial \beta}{\partial \mathbf{d}} = \frac{-1}{\phi\left(\Phi^{-1}(\hat{P})\right)} \frac{\partial \hat{P}}{\partial \mathbf{d}}. \tag{26}$$

It has to be noted that the axis orthogonal simulation is based on the assumption that only one MPP exists for each limit state function. Hence axis orthogonal simulation will not be very effective in computing probabilities of failure for cases with multiple MPPs. A directional simulation technique is a better choice for such class of problems. In directional simulation, the samples are generated in polar co-ordinates in **u** space and the samples are projected onto the limit state surface radially. If the samples are uniformly distributed in polar co-ordinates then one can obtain good estimates of probabilities of failure for limit states with multiple MPPs. But this technique would require lot more simulations to be able to get good accuracies in probabilities of failure than axis orthogonal simulation for limit states with single MPPs.

## 4 Approximate MCS-based RBO methodology

In this section, a new RBO methodology developed in this investigation is presented. This method uses approximate MCS techniques. The MCS-based reliability analysis could use exact limit state function evaluations but this will be very expensive for problems with many random variables and design variables. Hence the main goal of the current study is to reduce this computational expense. Approximation concepts are used in the approach presented herein to address this issue. In this study, approximations of the limit state functions are constructed, which are used to perform an approximate MCS-based RBO. This is performed in an iterative fashion. The approximate MCS-based RBO methodology presented here serves as a refinement of results obtained from a FORM-based RBO approach. The FORM-based RBO is used in the current approach to construct initial limit state approximations. It is important that the FORM-based RBO be successful which basically requires that the computation of MPP be performed using robust optimization algorithms (e.g. SQP). It is also assumed that extreme cases such as the existence of multiple MPPs do not occur for the application problems under consideration. The details of the main steps of the approximate MCS-based RBO methodology follow.

1. *FORM-based RBO*: First, a FORM-based RBO, that solves Equations (1–4), is performed with an initial design, $\mathbf{d}^{\text{init}}$ and with reliability constraints on component reliability indices based on FORM. This requires computation of MPPs and sensitivities of reliability indices with respect to **d** during each iteration. The

FORM-based RBO is used to provide a good estimate of initial design for the MCS-based RBO to be performed iteratively in steps 3–5. The result obtained from FORM-based RBO be denoted as $\mathbf{d}^0$.

2. *Initial Limit State Approximations*: Next, initial approximations for all limit state functions are created. Each limit state approximation is constructed at its MPP in $\{\mathbf{x}, \boldsymbol{\eta}\}$ space, as presented in Oakley et al. (1998). One of the motivations to construct the approximations in $\{\mathbf{x}, \boldsymbol{\eta}\}$ space as opposed to approximations in $\{\mathbf{u}, \boldsymbol{\eta}\}$ space is that for applications like structural optimization problems, certain classes of approximation functions are known to represent structural responses fairly accurately and hence it may be easier to construct these approximations in $\{\mathbf{x}, \boldsymbol{\eta}\}$ space. Moreover, by constructing limit state approximations in $\{\mathbf{x}, \boldsymbol{\eta}\}$ space, the effect of non-linearity of the transformation $\mathbf{T}$ can be captured. In the work presented here, the initial limit state approximations are constructed using the limit state function and sensitivity information generated during each iteration of the FORM-based RBO. The subscript for $g^R$ is dropped here in this section for convenience. It is implied that the procedures presented in this step and step 5 need to be performed for each limit state function. The following steps are carried out to obtain the initial limit state approximations:

   a. Start at $k = 1$. At the $k$th iteration of the FORM-based RBO, let $\boldsymbol{\eta}^k$ and $\boldsymbol{\theta}^k$ be the values of the deterministic design variable and distribution parameter vectors respectively. Let $\mathbf{u}^{*,k}$ and $\mathbf{x}^{*,k} = \mathbf{T}^{-1}(\mathbf{u}^{*,k}, \boldsymbol{\theta}^k)$ be the MPPs in $\mathbf{u}$ and $\mathbf{x}$ space, respectively. Let $\mathbf{w} = \{\mathbf{x}, \boldsymbol{\eta}\}$ and $\mathbf{w}^k = \{\mathbf{x}^{*,k}, \boldsymbol{\eta}^k\}$.
   b. A quadratic approximation, $\tilde{g}^{R,k}(\mathbf{w})$, of the following form is constructed:

$$\tilde{g}^{R,k}(\mathbf{w}) = g^{R,k} + \nabla_w g^{R,k}(\mathbf{w} - \mathbf{w}^k) + \frac{1}{2}(\mathbf{w} - \mathbf{w}^k)^T \mathbf{H}^k (\mathbf{w} - \mathbf{w}^k).$$

   In the above equation, $g^{R,k}$ and $\nabla_w g^{R,k}$ are the known value and sensitivity of $g^R$ at $\mathbf{w}^k$ respectively, and $\mathbf{H}^k$ is the unknown Hessian of the quadratic approximation. The Hessian is obtained using a variable metric algorithm, that is used for updating Hessians in optimization algorithms based on Quasi-Newton methods. A Symmetric Rank 1 (SR1) update algorithm (Nocedal and Wright, 1999) is used in this work. SR1 is known to generate Hessians accurately compared to other variable metric algorithms such as Broyden-Fletcher-Goldfarb-Shanno (BFGS) algorithm. This update is essentially a two-point update, where the Hessian is constructed by matching the exact sensitivities at previous iteration, i.e. $\nabla_w \tilde{g}^{R,k}(\mathbf{w}^{k-1}) = \nabla_w g^{R,k-1}$. The update is given by the following equation:

$$\mathbf{H}^k = \mathbf{H}^{k-1} + \frac{(\mathbf{q}^k - \mathbf{H}^{k-1}\mathbf{s}^k)(\mathbf{q}^k - \mathbf{H}^{k-1}\mathbf{s}^k)^T}{\mathbf{s}^{kT}(\mathbf{q}^k - \mathbf{H}^{k-1}\mathbf{s}^k)}, \tag{27}$$

   where $\mathbf{q}^{kT} = \nabla_w g^{R,k} - \nabla_w g^{R,k-1}$ and $\mathbf{s}^k = \mathbf{w}^k - \mathbf{w}^{k-1}$. The initial guess for the Hessian, $\mathbf{H}^0$, is taken as zero matrix. The update is performed only if $|\mathbf{s}^{kT}(\mathbf{q}^k - \mathbf{H}^{k-1}\mathbf{s}^k)| > \varepsilon_1$. The choice of $\varepsilon_1$ is important. The choice of a small value for $\varepsilon_1$ could result in large changes in the Hessians for small

changes in the design and consequently result in poor approximations. This was noticed in the second test problem and a choice of $\varepsilon_1 = 10^{-3}$ produced good results for the test cases considered herein. The choice of $\varepsilon_1$ can be made based on the magnitude of $\|\mathbf{s}^k\|$. A relative version of the update scheme can be used for this purpose such that the update is performed only if $|\mathbf{s}^{kT}(\mathbf{q}^k - \mathbf{H}^{k-1}\mathbf{s}^k)| > \varepsilon_1 \max(1, \|\mathbf{s}^k\|)$ and a typical value of $\varepsilon_1 = 10^{-6}$ can be used. Such an update scheme would prevent the updates from happening for very small changes in design.

c. Let $K$ be the number of iterations taken by the FORM-based RBO. If $k < K$, repeat steps 2 and 3, else, stop; the approximation for each limit state after the FORM-based RBO is $\tilde{g}^{R,K}$.

It has to be noted that the approximation type is not limited to quadratic and additional sampling can be performed to build these approximations. In the test problems considered, the SR1 variable metric algorithm was successful in giving good approximations and hence is presented here. Moreover, the SR1 update is quite simple to implement. It also should be noted that the limit state approximations being created during every iteration of the FORM-based RBO can also be used to perform approximate FORM analysis to reduce computational costs. This was not done in the current study primarily because the main focus here is to reduce the computational cost associated with the MCS-based RBO. Then $\tilde{\mathbf{g}}^{R,K}$ obtained from steps (a)–(c) is set as the initial approximation for the following iterative phase of the methodology, which starts at the iteration counter $j = 0$.

3. *Approximate MCS-based RBO*: With $\mathbf{d}^j$ as the starting point, perform an approximate MCS-based RBO, that solves Equations (1)–(4), using limit state approximations, i.e. $\tilde{\mathbf{g}}^{R,K+j}$, for the computation of $\mathbf{g}^{\text{rbo}}$, and using exact evaluations for $f$ and $\mathbf{g}^D$. The computations of MCS reliability constraints during this RBO involve finding MPPs and computing $\hat{P}$ and $\frac{\partial \hat{P}}{\partial \mathbf{d}}$ for each limit state approximation using axis orthogonal simulation. The sampling density function $h_{\mathbf{V}}$ is chosen as standard normal. The seeds of the random number generator and number of samples are kept fixed throughout this approximate RBO phase to reduce the discontinuities in probability of failure. Additional move-limit constraints can be imposed on $\mathbf{d}$, i.e. replace Equation (4) by $-\Delta \leq \mathbf{d} - \mathbf{d}^j \leq \Delta$, where $\Delta$ are the move-limits. Let the solution obtained from the approximate RBO be denoted as $\mathbf{d}^{j+1}$.
4. *Convergence Check*: The convergence is achieved if $\|\mathbf{d}^j - \mathbf{d}^{j+1}\| \leq \varepsilon_2$. $\varepsilon_2$ is set as $10^{-3}$ in the current study. If the convergence is achieved, stop, otherwise proceed to next step. $\varepsilon_2$ needs to be chosen based on the magnitudes of the design variables. A relative version of the convergence criteria can be used where the convergence is achieved if $\|\mathbf{d}^j - \mathbf{d}^{j+1}\| \leq \varepsilon_2 \max(1, \|\mathbf{d}^j\|)$. Many alternative convergence criteria involving the relative change of cost function, the norm of the gradient of the cost function and others that are typically used in gradient-based optimizers can be used to supplement or replace the current criteria.
5. *Update Limit State Approximations*: The limit state approximations are updated in the same fashion as described in step 2. To update the approximations, an exact MPP search corresponding to each limit state function, $g^R$, is performed at $\mathbf{d}^{j+1}$

to obtain $\mathbf{w}^{K+j+1}$, $g^{R,K+j+1}$, and $\nabla_w g^{R,K+j+1}$. Using this information and the previous Hessian, $\mathbf{H}^{K+j}$, one can obtain an updated Hessian, $\mathbf{H}^{K+j+1}$, from the SR1 update given by Equation (27). The updated Hessian can be substituted in Equation (27) to obtain the updated limit state approximation, $\tilde{g}^{R,K+j+1}$. After the approximations have been updated, increment $j$ by 1 and go to step 3.

## 5 Implementation studies

The approximate MCS-based RBO methodology and an exact MCS-based RBO method (for comparison purposes) were implemented for two test problems. The exact MCS-based RBO method was performed by solving Equations (1–4) with the optimum design obtained from a FORM-based RBO as the starting design. In the rest of this section, the approximate MCS-based RBO methodology will be referred to as the approximate approach and the exact MCS-based RBO will be referred to as the exact approach. The first problem is an analytic test problem and the second problem is a control-augmented-structure problem. The methodology was implemented in Matlab. The Sequential Quadratic Programming (SQP) subroutine was used to perform all the optimizations including the calculation of MPPs. The required component reliability indices for all the limit state functions for both FORM-based RBO and MCS-based RBO were set at 3.0 for both the test problems.

### 5.1 Analytic test problem

There are 2 design variables, $d_1, d_2$ and one parameter, $p$, in the analytic test problem. There are two random variables, $X_1$ and $X_2$. There are two limit state functions and one deterministic constraint. The details of the problem are as follows:

$$
\begin{aligned}
\text{Cost Function:} \quad & f = d_1^2 + y_1(d_1, p, d_2) + e^{-y_2(d_1,p,d_2)}. \\
\text{Limit state functions:} \quad & g_1^R = y_1(X_1, X_2, \eta)/2 - 1, \\
& g_2^R = X_1 + 1.5\eta - 0.5X_2 - 2.5. \\
\text{Constraints:} \quad & g_i^{\text{rbo}} = \beta_i - 3.0 \quad \text{for } i = 1, 2, \\
& g^D = y_2(d_1, p, d_2)/2 - 1, \\
\text{where} \quad & d_1 = \mu_{X_1}, \quad p = \mu_{X_2} = 0 \quad \text{and} \quad d_2 = \eta. \\
\mathbf{d} \text{ bounds:} \quad & 0 \le d_1 \le 10, \quad 0 \le d_2 \le 10.
\end{aligned}
$$

$y_1$ and $y_2$ are obtained by solving the following system of coupled equations:

$$
\begin{aligned}
y_1(x_1, x_2, \eta) &= x_1^2 + \eta - 0.2y_2(x_1, x_2, \eta), \\
y_2(x_1, x_2, \eta) &= \sqrt{y_1(x_1, x_2, \eta)} + x_1 + x_2.
\end{aligned}
$$

$X_1$ and $X_2$ are chosen as independent and normal random variables with standard deviation 0.5 each. $g_1^R$ is a nonlinear function and $g_2^R$ is a trivial linear function.

**Table 1** The initial design and RBO designs obtained using FORM-RBO, approximate and exact MCS-RBO approaches for Test Problem 1 are shown

| | | | MCS-RBO designs | |
|---|---|---|---|---|
| | Initial design | FORM-RBO design | Approximate | Exact |
| $d_1$ | 4.00 | 0.45 | 0.47 | 0.47 |
| $d_2$ | 5.00 | 2.58 | 2.54 | 2.54 |
| $f$ | 35.32 | 2.73 | 2.71 | 2.71 |
| $g^D$ | 3.20 | **0.00** | **0.00** | **0.00** |
| $\beta_1$ | | **3.0** (MCS 3.4) | **3.0** | **3.0** |
| $\beta_2$ | | 3.27 (MCS 3.27) | 3.17 | 3.17 |
| Analysis calls | | 1,300 | 1,500 | 62,700 |

*Note*. FORM-RBO gives a conservative design. The final designs obtained from approximate and exact approaches are close and the former requires 40 times fewer analysis calls.

In both the proposed approximate approach and the exact approach, axis orthogonal simulations using 100 samples for both limit state functions were performed. The samples were generated according to standard normal sampling density functions. The seed for the random number generator used to generate the samples was set to the same initial state for all the iterations. The initial design, the FORM-based RBO design and the final designs obtained from the approximate and exact MCS-based RBO approaches are shown in Table 1. Table 1 also presents the reliabilities for the FORM-RBO and MCS-RBO designs. In the column representing the FORM-RBO results, the FORM estimate of the reliability for each limit state function is presented and an MCS estimate at this design is also provided in parentheses. The values corresponding to the active constraints are shown in bold.

In both the FORM-based RBO design and the MCS-based RBO design the reliability constraints for $g_1^R$ and $g^D$ were active. Though the FORM-based RBO design and the final design obtained from the MCS-based RBO appear to be similar, the MCS reliability indices were significantly different for these two designs. The MCS reliability index for $g_1^R$ was 3.4 at the FORM-based RBO design. The probability of failure corresponding to a reliability index of 3.4 is 4 times lower than the probability corresponding to the required reliability index of 3.0. Hence the FORM-based RBO design was conservative and the MCS-based RBO methodology was able to lower the reliability index to the desired value and was also able to lower the cost function, $f$. The FORM result is conservative because the failure domain for $g_1^R$ is convex in standard space for the random variable distributions considered. It will be difficult to say if this will be the case for other distributions. The final design obtained using the approximate MCS-based RBO approach was identical to the result obtained from the exact approach. The accuracies of the MCS reliability indices were verified by performing confirmatory runs where the axis orthogonal simulations were performed with larger number of samples. The exact approach that used exact limit state evaluations required as many as 62,700 analysis calls whereas the approximate approach required only 1,500 analysis calls (excluding confimatory runs), of which 1,300 analysis calls were taken by the FORM-based RBO. The number of analysis calls required was 40 times lower than the exact approach considering both the FORM and the approximate

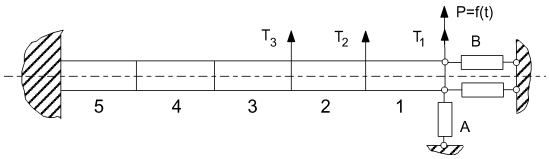


**Fig. 4** Control augmented structure

MCS-based RBO. The number of analysis calls was almost 300 times lower than the exact approach excluding the analysis calls required by the FORM-based RBO.

## 5.2 Control-augmented-structures problem

Figure 4 shows the control-augmented-structure as presented by Sobieszczanski-Sobieski et al. (1990). The structure is a 5 element cantilever beam, numbered 1–5 from the free end to the fixed end, as shown in the Figure 4. There are three static loads $T_1$, $T_2$ and $T_3$ and a dynamic force $f(t)$, which is a ramp function. Controllers A and B are designed as an optimal Linear Quadratic Regulator. This is a coupled problem since the design of the controllers depend on the dynamic characteristics of the structure, which in turn requires the weight of the controllers that are modelled as a lumped mass on the structure. The cost function for this problem is the total weight of the beam and the controllers.

There are 11 design variables in this test problem. The design variables and design variable bounds for this test problem are given below as,

$$\begin{aligned}
\mathbf{d} &= [b_1, b_2, b_3, b_4, b_5, h_1, h_2, h_3, h_4, h_5, c]^T, \\
3 \leq b_i &\leq 36, \qquad i = 1, \ldots, 5, \\
3 \leq h_i &\leq 36, \qquad i = 1, \ldots, 5, \\
0.01 \leq c &\leq 0.06,
\end{aligned}$$

where $b_i$ and $h_i$ are the breadth and height of the $i$th element respectively and $c$ is the damping matrix to stiffness matrix ratio (scalar).

For this problem, the following limit state functions were selected:

$$\begin{aligned}
g_1^R &= 1 - \left(\frac{dl_1}{50}\right)^2, \\
g_2^R &= 1 - \left(\frac{dr_1}{0.2}\right)^2, \\
g_{2+i}^R &= 1 - \frac{\sigma_i}{\sigma_a}, \qquad i = 1, \ldots, 5,
\end{aligned}$$

where $dl_1$ and $dr_1$ are the lateral and rotational static displacements of element 1 respectively, and $\sigma_i$ is the maximum static stress in element $i$. The random variables for this problem are the ultimate static stress, $\sigma_a$, density, $\rho$, modulus of elasticity, $E$, and loads $T_1$, $T_2$ and $T_3$. The distribution properties of the random variables are given in Table 2. The distribution functions for $\sigma_a$, $\rho$ and $E$ were taken as lognormal

**Table 2** Test problem 2-random variables

| | Distribution | Mean | Std. Dev. |
|---|---|---|---|
| $\sigma_a$ (psi) | Lognormal | 30,000 | 3,000 |
| $\rho$ $(lb/in^3)$ | Lognormal | 0.1 | 0.01 |
| $E$ (ksi) | Lognormal | 10,500 | 1,050 |
| $T_1$ (lbs) | Uniform | 1,000 | 400 |
| $T_2$ (lbs) | Uniform | 5,000 | 2,000 |
| $T_3$ (lbs) | Uniform | 1,000 | 400 |

since these are non-zero quantities and the coefficients of variation were set at 0.1. $T_1$, $T_2$ and $T_3$ were taken to be uniformly distributed with coefficients of variation set at 0.4, which introduced considerable non-linearity in the problem that resulted in a significant difference between the FORM and MCS reliabilities. It has to be noted that the uncertainties were chosen to be independent for convenience of implementation. In a real scenario, the uncertainties related to material properties could be dependent. The purpose of this work was to illustrate the computational efficiency of the proposed approximate MCS-based RBO methodology over an exact approach, primarily. But it has to be noted that the reliability techniques such as FORM and the MCS technique used in this work can be straightforwardly extended to problems with dependent random variables because the Rosenblatt transformation can handle dependent random variables (Rosenblatt, 1952). The reliability constraints for this problem are given by the following equation:

$$g_i^{\text{rbo}} = \beta_i - 3.0 \quad \text{for } i = 1, \ldots, 7.$$

In both the proposed approximate approach and the exact approach, axis orthogonal simulations using 500 samples for all the limit state functions were performed. The samples were generated according to standard normal sampling density functions. The seed for the random number generator used to generate the samples was set to the same initial state for all the iterations in the approximate RBO. The initial design, the FORM-based RBO design and the final designs obtained from the approximate and exact MCS-based RBO approaches are shown in Table 3. Table 3 also presents the reliabilities for the FORM-RBO and MCS-RBO designs. In the column representing the FORM-RBO results, the FORM estimate of the reliability for each limit state function is presented and an MCS estimate at this design is also provided in parentheses. The values corresponding to the active constraints are shown in bold. The initial design was selected as the result obtained from a deterministic optimization problem similar to the RBO problem but with no reliability constraints and all limit state functions treated as deterministic constraints. At this design, the limit state function $g_1^R$ was active and the reliability indices for all the limit state functions were way below the required reliability index of 3.0 and were close to zero (50% probability of failure) for certain limit state functions.

The final design obtained using approximate MCS-based RBO approch was similar to the result obtained using the exact approach. At the FORM-based RBO design and MCS-based RBO design, the reliability constraints for the static stress constraints, i.e. $g_i^R, i = 3, \ldots, 7$, were active. It can be seen that the FORM-based RBO design corresponds to a heavier structure than the final design. In the FORM design, the

**Table 3** The initial design and RBO designs obtained using FORM-RBO, approximate and exact MCS-RBO approaches for test problem 2 are shown

| | | | MCS-RBO designs | |
|---|---|---|---|---|
| | Initial design | FORM-RBO design | Approximate | Exact |
| $b_i, i = 1, \ldots, 5$ | 3.00 | 3.00 | 3.00 | 3.00 |
| $h_1$ | 3.70 | 3.74 | 3.70 | 3.70 |
| $h_2$ | 7.04 | 9.67 | 9.48 | 9.48 |
| $h_3$ | 9.81 | 13.56 | 13.30 | 13.30 |
| $h_4$ | 12.00 | 16.58 | 16.26 | 16.26 |
| $h_5$ | 13.84 | 19.14 | 18.77 | 18.76 |
| $c$ | 0.06 | 0.06 | 0.06 | 0.06 |
| $f$ | 1493.9 | 1926.6 | 1894.3 | 1894.1 |
| $\beta_1$ | | 4.79 (MCS 5.07) | 4.61 | 4.60 |
| $\beta_2$ | | 3.33 (MCS 3.63) | 3.26 | 3.26 |
| $\beta_3$ | | **3.00** (MCS 3.18) | **3.00** | **3.00** |
| $\beta_4, \beta_5, \beta_6$ | | **3.00** (MCS 3.29) | **3.00** | **3.00** |
| $\beta_7$ | | **3.00** (MCS 3.30) | **3.00** | **3.00** |
| Analysis calls | | NA | $\approx 2,600$ | $\approx 273,000$ |

*Note*. FORM-RBO gives a conservative design. The final designs obtained from approximate and exact approaches are close and the former requires 100 times fewer analysis calls.

MCS-computed reliability indices for the static stress constraints were as high as 3.3. The probability of failure corresponding to a reliability of 3.3 is more than 2.5 times lower than the probability corresponding to the required reliability index of 3.0. Hence the design was conservative. As mentioned in the previous subsection, the FORM estimates are probably conservative for this implementation study too, because the failure domains are convex in standard space for the random variable distributions considered. This need not necessarily be true for other random variable distributions. It was noted for this problem that the choice of $\varepsilon_1$ in SR1 update scheme greatly influenced the accuracy of initial limit state approximation for $g_1^R$ and consequently the prediction of the corresponding MCS reliability index, which was extremely low. Moreover, the accuracy of the limit state approximation for $g_1^R$ deteriorated when large design changes were made during the approximate MCS-based RBO phase, which consequently led to extremely high reliability estimates. Hence the move-limits for the approximate MCS-based RBO were reduced to $\pm 0.5\%$ of the design variable bounds, which forced the approximate MCS-based RBO to make small design changes. For this choice of move-limit size, the reliability index for $g_1^R$ did not exhibit large variations between iterations and smoothly converged to the reliability index obtained from the exact MCS-based RBO approach. The approximate MCS-based RBO could predict the reliability indices fairly well for other limit states and the accuracies in the reliability indices were insensitive to the choice of move-limit size or $\varepsilon_1$. The acccuracies of the MCS reliability indices were verified by performing confirmatory runs where the axis orthogonal simulations were performed with larger number of samples. The approximate MCS-based RBO methodology required about 2,600 finite element analysis calls (excluding confirmatory runs), whereas the exact MCS-based RBO approach that used exact limit state evaluations required as many as 273,000 finite element analysis calls.

The proposed methodology required 100 times fewer analysis calls than the exact approach.

## 6 Conclusions

An approximate MCS-based RBO methodology that uses limit state approximations has been developed and successfully implemented for two test problems. A conditional-expectation-based MCS technique is better suited for RBO than an indicator-based MCS and hence it was used for the approximate RBO in the RBO methodology presented in this study. For comparison purposes, results using exact calculations of the limit states are also presented for both these test problems. The SR1 update algorithm typically provided accurate limit state approximations that captured the trends of the limit state function. For both of the test problems, the proposed methodology required nearly two orders of magnitude fewer analysis calls than an approach that required exact evaluations of the limit states and this dramatically illustrates the potential of the methodology.

It is expected that the accuracy of the limit state approximations is very critical for the success of this methodology. The current methodology provides no way of determining directly the accuracy or goodness of the limit state approximations that are constructed using SR1 algorithm. The limit state approximations can be computed using other techniques such as those based on Design of Experiments, where statistical goodness-of-fit measures such as $R^2$ can be used. This can be used in tandem with a move-limit management strategy to further increase the robustness of the methodology. In the proposed methodology, FORM-based RBO uses exact limit state calculations. One could employ limit state approximations in FORM-based RBO to further reduce limit state evaluations or analysis calls. The axis orthogonal simulation technique used in the current study does not effectively calculate probabilities of failure for problems with multiple MPPs since the simulations are performed after the calculation of an MPP. Other MCS techniques such as directional simulation need to be explored to address such problems. The current implementation also assumes that only single solution exists for the projection of each sample on the limit state. The implementation can be improved to account for multiple solutions that may arise in non-linear examples. In the current study, it is assumed that the joint probability distributions are available for the uncertainties. Typically the joint distributions are difficult to obtain and only partial information such as correlations are available along with individual marginal distributions. The MCS techniques also need to be extended for such problems of practical importance. One possible approach to address such problems would be to use the Morgenstern and Nataf joint distribution models that can be easily evaluated in terms of known marginals and correlation coefficients (Liu and Der Kiureghian, 1986).

**Acknowledgements** The authors would like to acknowledge the support provided by the Center for Applied Mathematics and Aerospace and Mechanical Engineering Department at University of Notre Dame. The authors would like to acknowledge the contributions made by Dr. Victor M. Pérez, former Graduate Research Assistant at University of Notre Dame, currently working at General Electric, Mexico

## References

Bjerager P (1989) Methods for structural reliability computations. Technical report, University of California, Berkeley. Lecture Notes for the course structural reliability: methods and applications

Ditlevsen O, Madsen HO (1996) Structural reliability methods. John Wiley & Sons, Inc

Enevoldsen I, Sørensen JD (1993) Reliability-Based Optimization of series systems of parallel systems. J Structural Eng 119(4):1069–1084

Enevoldsen I, Sørensen JD (1994) Reliability-Based Optimization in structural engineering. Structural Safety 15(3):169–196

Engelund S, Rackwitz R (1993) A benchmark study on importance sampling techniques in structural reliability. Structural Safety 12:255–276

Grandhi RV, Wang L (1998) Reliability-based structural optimization using improved two-point adaptive nonlinear approximations. Finite Elements in Analysis and Design 29

Haldar A, Mahadevan S (2000) Probability, reliability and statistical methods in engineering design. John Wiley & Sons, Inc

Kirjner-Neto C, Polak E, Der Kiureghian A (1998) An outer approximations approach to reliability-based optimal design of structures. J Optimiz Theor Appl 98(1):1–16

Kuschel N, Rackwitz R (1997) Two basic problems in reliability-based structural optimization. Math Meth Operations Res 46(3):309–333

Liu P-L, Der Kiureghian A (1991) Optimization algorithms for structural reliability. Structural Safety 9:161–177

Liu P-L, Der Kiureghian A (1986) Multivariate distribution models with prescribed marginals and covariances. Prob Eng Mech 1(2):105–112

Maes MA, Breitung K, Dupuis DJ (1993) Asymptotic importance sampling. Structural Safety 12:167–186

Nocedal J, Wright SJ (1999) Numerical optimization, springer series in operations research. Springer

Oakley DR, Sues RH, Rhodes GS (1998) Performance optimization of multidisciplinary mechanical systems subject to uncertainties. Prob Eng Mech 13(1):15–26

Oberkampf WL, DeLand SM, Rutherford BM, Diegert KV, Alvin KF (2000) Estimation of total uncertainty in modeling and simulation. Technical Report SAND2000-0824, Sandia National Laboratories

Rosenblatt M (1952) Remarks on a multivariate transformation. The Annals Math Stat 23(3):470–472

Sobieszczanski-Sobieski J, Bloebaum CL, Hajela P (1990) Sensitivity of control-augmented structure obtained by a system decomposition method. AIAA J 29(2):264–270

Sørensen JD, Enevoldsen I (1993) Sensitivity weaknesses in application of some statistical distributions in first order reliability methods. Structural Safety 12:315–325

Tu J, Choi KK (1999) A new study on reliability-based design optimization. J Mech Design, Trans ASME 121:557–564